Particle Hemodynamics Analysis after Coronary Angioplasty

S.I. Bernad, A.F. Totorean, V.F. Vinatu, R.F. Susan-Resiga

Abstract—**The resistance to flow through a stenosis caused by viscous friction, flow separation, turbulence, and eddies at the site of the stenosis results in energy loss. Energy loss produces pressure loss distal to the stenosis and thus a pressure gradient across the narrowed segment. Assessment of shear stress, along with percent stenosis, in arterial lesions might prove to be a valuable diagnostic tool to identify patients at risk of developing acute platelet thrombus formation in stenosed arteries. The goal is to provide a logical approach to the use of coronary physiological measurements to assist both clinicians and investigators in improving patient care.**

Index Terms—**hemodynamic parameters, fractional flow reserve, particle motion, vascular remodelling.**

I. INTRODUCTION

Coronary atherosclerosis is focal and eccentric, and each coronary obstruction progresses or regresses in an independent manner, including areas after percutaneous revascularization. Local hemodynamic factors are crucial to determine the evolution of coronary obstructions. The vascular endothelium is in a pivotal position to respond to the dynamic forces acting on the vessel wall owing to the complex 3D geometry of the artery. Fluid shear stresses elicit a large number of responses in endothelial cells. The response of genes sensitive to local hemodynamic forces likely leads to creation of a raised plaque; subsequent hemodynamic forces created by the plaque may lead to a cycle of cellular recruitment and proliferation, lipid accumulation, and inflammation.

When atherosclerosis develops, advanced lesions form first in some regions with adaptive intimal thickening. In humans, the topographic distribution of eccentric intimal thickening and of advanced atherosclerotic lesions is similar in the coronary arteries [1], the internal carotid artery at the level of the carotid sinus [2], and the aorta.

S.I. Bernad, Romanian Academy – Timisoara Branch, Bd. Mihai Viteazul 24, Ro-300223, Timisoara, Romania, Tel/Fax: +4-0256-403692, (e-amail: sbernad@mh.mec.upt.ro)

A.F. Totorean, "Politehnica" University Timisoara, Department of Medical Engineering, Bd. Mihai Virteazul 1, RO-300222, Timisoara, Romania, (e-mail: alin_totorean@yahoo.com).

V.F. Vinatu, "Politehnica" University Timisoara, Department of Medical Engineering, Bd. Mihai Virteazul 1, RO-300222, Timisoara, Romania, (e-mail: vlad@mea-edu.ro).

R.F. Susan-Resiga, "Politehnica" University Timisoara, Department Hydraulic Machinery, Bd. Mihai Virteazul 1, RO-300222, Timisoara, Romania, (e-mail: resiga@mh.mec.upt.ro).

A complete description of hemodynamics within a particular vessel or lesion requires knowledge of the pattern of blood velocities within the flow [3], [4]. The latter depends on the geometry and mechanical properties of the vascular wall, an overall pressure difference, and the rheological characteristics of blood (viscosity, density). Knowledge of the pattern of velocities near the vessel wall allows evaluation of WSS values and thus may provide indications for estimating the risk for development and progression of atherosclerosis, rupture of atherosclerotic plaques, and hemorrhage associated with cerebral aneurysms and arteriovenous malformations. At the earlier stages of research in this area, contradictory data were reported that had associated both high and low WSS values with atherosclerosis [5], [6].

Wall shear stress (WSS) expresses the force per unit area exerted by a solid boundary on a fluid in motion (and vice-versa) in a direction on the local tangent plane. Currently, issues related to WSS distribution in arterial flow are receiving attention because of emerging evidence that it is associated with vascular disease and, specifically, atherosclerosis. It is now well established that WSS plays a significant role in endothelial homeostasis and the focal distribution of atherosclerotic lesions [7], [8].

In normal clinical practice, coronary arteries eligible for surgical revascularization are selected subjectively by visual estimation of stenosis severity, morphologic appearance of the lesion that may be judged as unfavorable for percutaneous coronary intervention (PCI), and the physician's personal preference.

Fractional flow reserve (FFR) calculated from coronary pressure measurements permits reliable assessment of the functional severity of a stenosis in a coronary artery. FFR of the coronary artery equals the ratio P_d/P_a at maximal hyperemia where P_a is the mean aortic pressure, measured by the guiding catheter, and P_d is the distal coronary pressure, measured by a pressure wire. FFR is the gold standard for physiologic stenosis severity, and a value below 0.75 indicates a functionally significant stenosis [9].

The goal here is twofold. On one hand, the pressure and particles distributions and WSS at the locations of constricted region are evaluated. On the other hand, the way in which the FFR is affected by the blood flow evolution during the cardiac cycle in stenosed region.

II. CONCEPTS AND TECHNIQUES

A. Computational geometry

A 3D computer model of a disease human coronary (Fig. 1) is obtained using data set presented by Banerjee et al. [10]

corresponding to the pacient with single vessel and single lesion coronary artery disease. Dimensions of the coronary stenosis after angioplasty is presented in Table I.

B. Numerical method

Unsteady flow Navier–Stokes equations for momentum and mass conservation were solved by a control volume finite element method implemented in FLUENT 6.3 (ANSYS-Fluent, ANSYS, Inc.). Calculation of local WSS is an integral part of the software based on partial differentiation of local velocity near wall perpendicular to the corresponding surface element (WSS $=\mu(\partial(\text{velocity})/\partial(\downarrow$ surface). For finite element numerical simulation the vessel volume was transformed to a mesh grid using the software Gambit 2.4.6 (ANSYS-Fluent, ANSYS, Inc.). A high mesh resolution near the walls was needed for accurate values of

WSS. Thus the mesh was refined in the near-wall region. A boundary layer consisting of four rows of prisms, with a growth factor of 1.2 (ratio between two consecutive layers near the wall) was generated.

Table 1. Dimensions for the stenotic sections

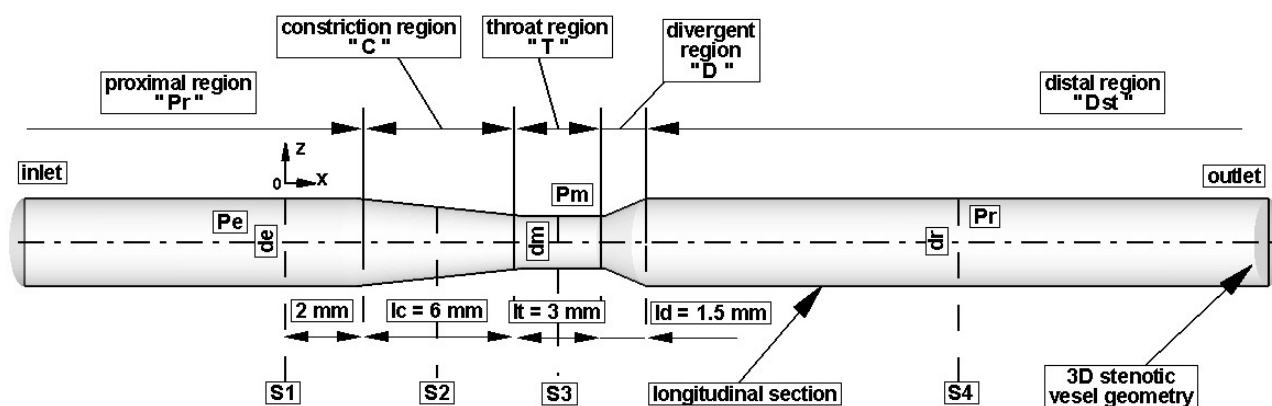| Geometrical parameters		Flow characteristics
$d_e = 0.003$ m	$l_c = 0.002$ m	$100 < \text{Re}_e < 400$
$d_m = 0.0018$ m	$l_t = 0.006$ m	$50 < Q < 150$
$d_r = 0.003$ m	$l_d = 0.0015$ m	
% diameter stenosis = 40 %		
% area stenosis = 64 %		

Figure 1. 3D reconstruction of the stenotic coronary vessel.

Unsteady turbulent flow was simulated presuming rigid motionless walls. A no-slip condition was assumed at the wall. The pressure value was imposed at the outlet. Blood was modelled as a Newtonian fluid with a kinematic viscosity of 3.5×10^{-6} m^2/s. A second order discretization scheme and a SIMPLEC model for pressure-flow coupling were used. The convergence criteria for relative errors in velocity components and pressure were set as 1×10^{-6}.
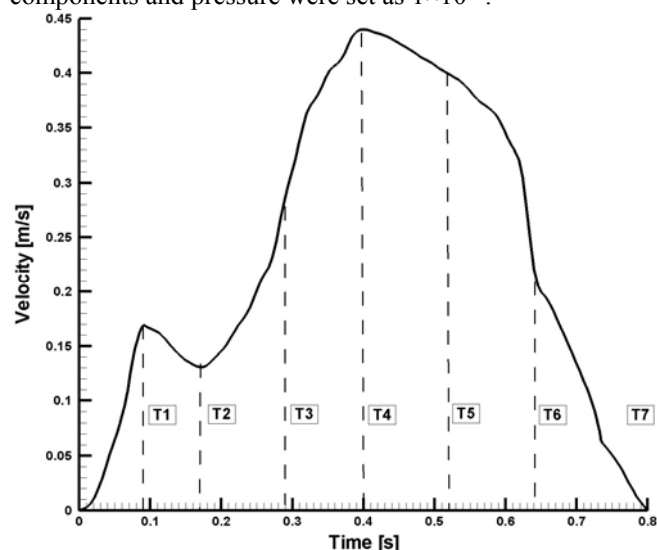

Figure 2. Coronary flow waveform.

Parabolic velocity profile was assumed at the inlet section. The mean flow rate for coronary artery derived from intravascular flow velocity measurements in the patient [10].

C. Hemodynamic diagnostic parameters

In normal clinical practice, coronary arteries eligible for surgical revascularization are selected subjectively by visual estimation of stenosis severity, morphologic appearance of the lesion that may be judged as unfavorable for percutaneous coronary intervention (PCI), and the physician's personal preference.
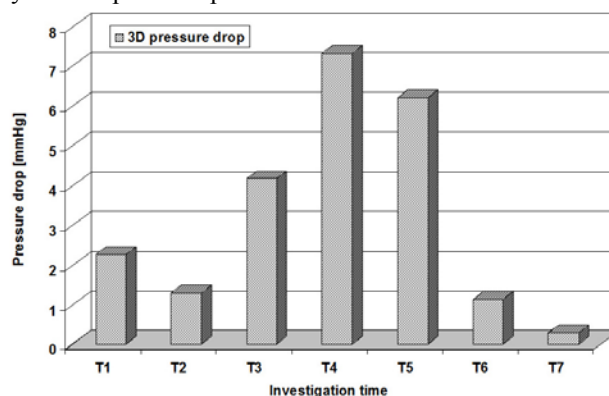

Figure 3. Coronary flow waveform.

Using this invasive pressure and flow measurement, various diagnostic parameters have been developed in current

clinical practice e.g. coronary flow reserve (CFR: the ratio of hyperemic flow to the basal flow) [11], trans-stenotic pressure drop [12], fractional flow reserve (FFR: the ratio of distal recovered pressure to the aortic pressure at hyperemia) [9].

III. RESULTS

A. Pressure variations

To understand the pressure–flow relationship, pressure variations across the stenosed artery have been evaluated. In Fig. 3 the pressure field drop along the vessel has been plotted covering the total investigated cardiac cycle.

For the three-dimensional vessel model, the non-uniform hemodynamic indicators for the investigated time T4=0.4 s, and T6=0.64 s, are shown in Fig. 4b and Fig. 5b. Lower WSS regions exist near the expansion wall and downstream of the expansion wall, coinciding with flow separation zones shown in Fig. 4b and 5b.
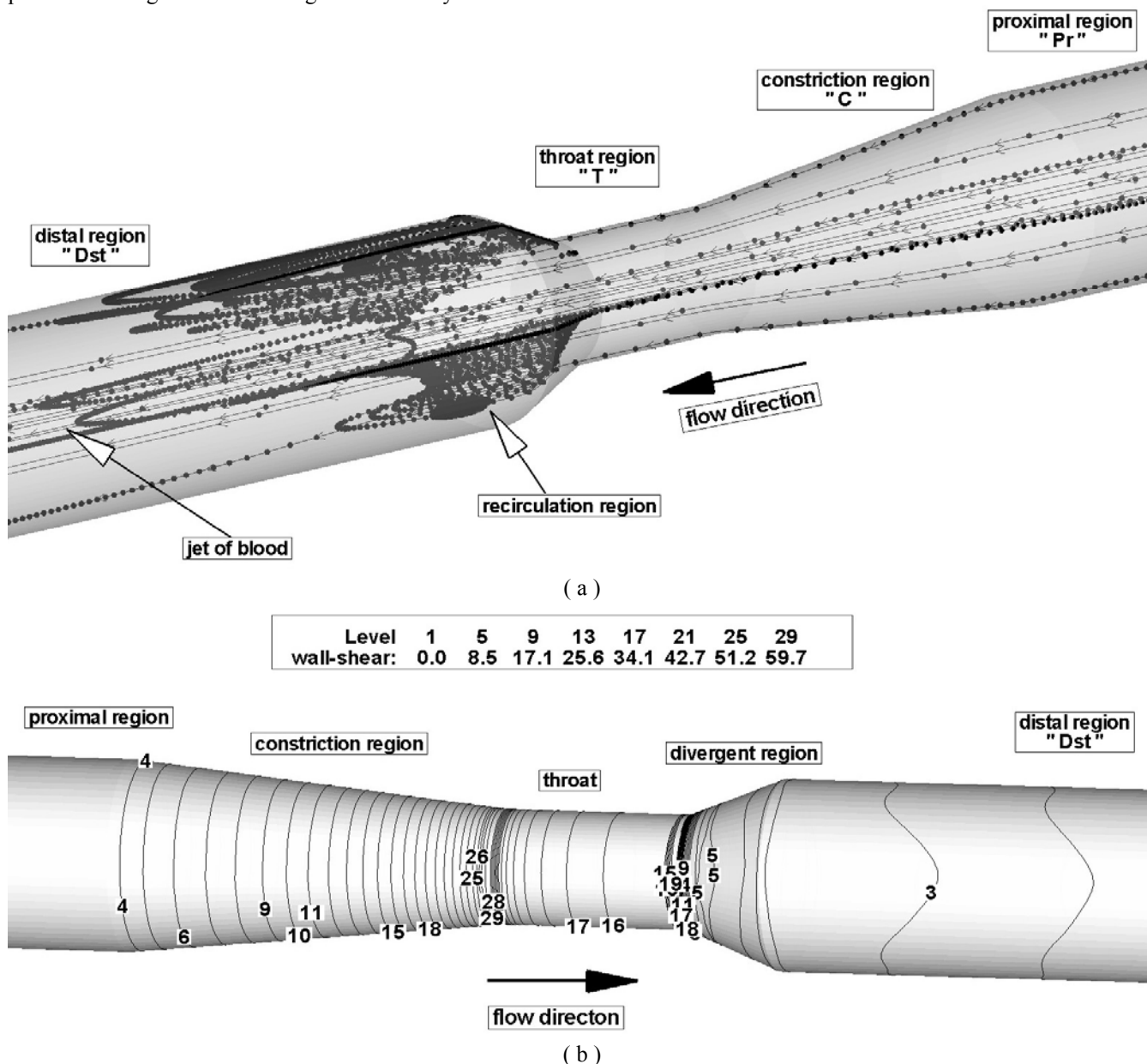

(a)

Level	1	5	9	13	17	21	25	29
wall-shear:	0.0	8.5	17.1	25.6	34.1	42.7	51.2	59.7

(b)

Figure 4. Particle motion (a) and contour plot of WSS magnitude (b) in the constricted region at the time T4=0.4 s.

The magnitude and direction of wall shear stress influence inflammatory processes in the vessels. Although the interaction of wall shear stress and inflammation involves a complicated cascade, slow and turbulent flow condition has been shown to induce gene expression of proinflammatory molecules in the endothelial cells [15], [16].

B. Particle trajectories

In this study, the disturbed flow structures and particle transport in the vicinity of axisymmetric expansions are simulated and possible links between disturbed flow indicators with particle transport and postoperative complications after percutaneous transluminal ballon coronary angioplasty (PTCA) are analyzed.

To study particle aggregation and deposition, near wall particle motion is observed, and particle deposition patterns for axisymmetric expansion geometries are compared with WSS distributions (Figs. 4 and 5). At time $T=T_0$, it is assumed that a large number of particles are distributed at the inlet section. 1,032 distributed particles are seeded for axisymmetric expansion geometries. The unsteady flow result shows the maxima of particle deposition near the time-averaged reattachment point (Figs. 4a and 5a) which coincides with the locations of WSS peaks (Figs. 4b and 5b). The results for axisymmetric particle deposition distribution are similar to those experimentally measured data from Karino et al. [17] and Pritchard et al. [18].

Streamlines (Figs. 4a and 5a) display a snapshot of the entire flow field at an instant in time, whereas particle pathlines trace the history of a particular fluid element through a region. Of interest are spherical particle that stay in a recirculation zone or can be assumed to "stick" when they come in contact with the wall. The non-uniform fluid mechanics (disturbed flow) lead to unusual pathlines as shown in Figs. 4a and 5a.
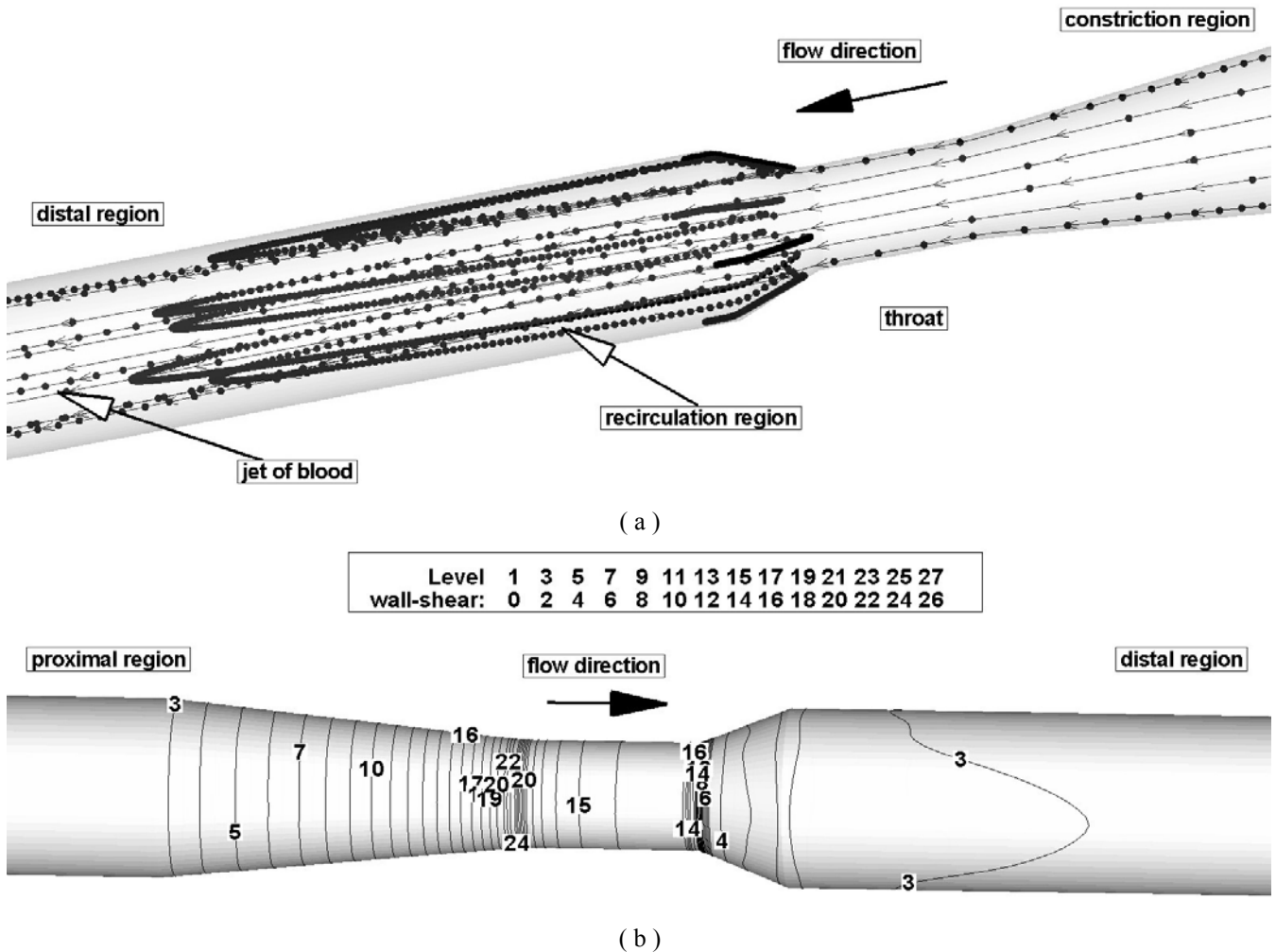

(a)

(b)

Figure 5. Particle motion (a) and contour plot of WSS magnitude (b) in the constricted region at the time T6=0.64 s.

IV. DISCUSSIONS

The particle motion plots provide quite similar flow patterns for both investigated time (T4 and T6), i.e. recirculation in the vicinity of the expansion wall, strong jet flow around the center line, prolonged recirculation during the decelerating systolic phase.

Stenoses and post-stenotic dilatations have led to acceleration and rapid deceleration, respectively, including a distortion of flow. Large recirculation regions found in the vicinity of the each constricted section. Post-stenotic deceleration of blood flow induces flow separation and recirculation zones.

Along the stenosed arterial wall, the shear stress (SS) varies significantly from point to point. The SS, very low outside the stenosis, suddenly increases with the narrowing diameter, and reaches a maximum at the beginning of the smallest diameter inside the stenosis (Fig. 4b and 5b). Increasing the amount of stenosis usually reduced the flow through the stenosis. However, due to the cubic dependence of shear on diameter, the overall effect is to increase the SS.

Parallel to the changes of WSS, the flow pattern was more variable and inconsistent in the vicinity of the constriction (Fig. 4a and 5b). Artery section constriction and post-constriction dilatations have led to acceleration and rapid deceleration, respectively, including a flow distortion.

The change of WSS throughout the cardiac cycle highly correlated to flow velocities. The WSS characterizes the forces that longitudinally act on the vessel wall. These forces were high when the blood flow parallel to the wall was fast.

The maximum WSS spatial variation was approximately 60 Pa in stenosed section (Fig. 4b) at the time T4 = 0.4 s, and the WSS maximum spatial variation is 26 Pa in stenosed section (Fig. 5b), corresponding to the investigated time T6=0.64 s.

Localized high stresses in the vessel wall have been found to relate to local disease development [19]. Furthermore, it has been indicated by numerous studies that fluid dynamics plays an important role in the initiation and development of atherosclerosis [20], [21] and it is possible that certain arterial motion may promote atherosclerosis by creating or exacerbating a pathogenic fluid dynamic environment.

Comparing hemodynamic changes throughout a cardiac cycle between a normal and an atherosclerotic vessel revealed that the arteriosclerotic wall contains more regions with WSS variations. Whereas in normal coronary arteries

the WSS remained low during phases of high flow velocity, the WSS was elevated in arteriosclerotic vessels, even at low flow velocities.

Parallel to the changes of WSS, the flow pattern was more variable and inconsistent in arteriosclerotic vessels. Stenoses and post-stenotic dilatations have led to acceleration and rapid deceleration, respectively, including a distortion of flow (Fig 4a and Fig. 5a).

The main function of wall pressure representing a map of the pressure inside the coronary artery is to push the blood into the capillaries and facilitate diffusion into the myocardium. The increased pressure drop (Table 2) in stenoses reflects the elevated energy needed to drive the flow through these regions. As shown in atherosclerotic coronary arteries, regions of flow acceleration were associated with high WSS.

Table 2. Mean pressure drop and mean pressure recovery during the cardiac cycle

Time [s]	Proximal pressure Pe [Pa]	Distal pressure Pr [Pa]	Pressure drop Pe - Pr [mmHg]	Pressure recovery Pr - Pm [mmHg]
T1	385	84	2.26	-0.35
T2	194	22	1.29	0
T3	614	57	4.18	0.46
T4	938	-39	7.33	1.52
T5	784	-44	6.21	1.35
T6	48	-104	1.14	0.95

FFR was calculated by the ratio Pr/Pe at steady-state maximum hyperemia, where Pr is the mean coronary pressure distal in the coronary artery and Pe is the mean aortic pressure, as described before [9]. FFR variations during the cardiac cycle are presented in Table 3.

Table 3. FFR variations during the cardiac cycle

Time [s]	Proximal pressure Pe [Pa]	Distal pressure Pr [Pa]	FFR
T1	385	84	0.21
T2	194	22	0.11
T3	614	57	0.09
T4	938	-39	0.04
T5	784	-44	0.05
T6	48	-104	2.1

Results from the flow computations are also presented as particle plots for the stenosed artery. During the simulation, massless particles are introduced into the flow domain at the inlet section. Fig. 6 shows the final particles distribution after one cardiac cycle.

V. CONCLUSION

Assessment of shear stress, along with percent stenosis, in arterial lesions might prove to be a valuable diagnostic tool to identify patients at risk of developing acute platelet thrombus formation in stenosed arteries. Computer flow models can be utilized in conjunction with human coronary angiography to study flow characteristics for plaques of different sizes and shapes in patients with stable and unstable angina.

Combined measurement of distal pressure and flow velocity, made possible by recent advancements in wire fabrication technology, not only yields a high diagnostic accuracy but also holds great potential for improved guidance of coronary interventions in the catheterization laboratory.
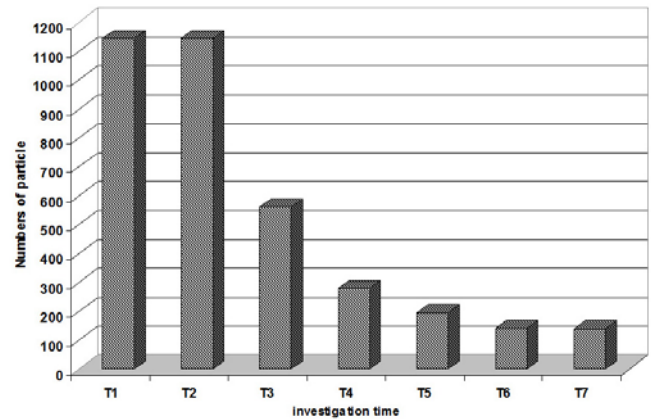

Figure 6. Particles distributions during the cardiac cycle.

APPENDIX

d_e - proximal vessel diameter [m]

d_m - throat minimal diameter [m]

d_r - distal vessel diameter [m]

l_c - length of converging section [m]

l_t - throat length [m]

l_d - length of diverging section [m]

P_e - mean proximal pressure [Pa]

P_m - mean pressure in the throat [Pa]

P_r - mean distal pressure [Pa]

REFERENCES

[1] H. C. Stary, "Evolution and progression of atherosclerotic lesions in coronary arteries of children and young adults", *Arteriosclerosis*, vol 9 (suppl I), 1989, pp: 19-32.

[2] C. K. Zarins, D. P. Giddens, B. K. Bharadvaj, V. S. Sottiurai, R. F. Mabon, S. Glagov, "Carotid bifurcation atherosclerosis: Quantitative correlation of plaque localization with flow velocity profiles and wall shear stress", *Circ Res*, vol 53, 1983, pp: 502-514.

[3] L. Goubergrits, K. Affeld, E. Wellnhofer, R. Zurbrugg, T. Holmer, "Estimation of wall shear stress in bypass grafts with computational fluid dynamics method", *Int J Artif Organs*, vol 24, 2001, pp: 145–51.

[4] B. K. Lee, H. M. Kwon, B. K. Hong, et al, "Hemodynamic effects on atherosclerosis-prone coronary artery: wall shear stress/rate distribution and impedance phase angle in coronary and aortic circulation", *Yonsei Med J*, vol 42, 2001, pp: 375–383.

[5] P. H. Stone, A. U. Coskun, Y. Yeghiazarians, et al, "Prediction of sites of coronary atherosclerosis progression: in vivo profiling of endothelial shear stress, lumen, and outer vessel wall characteristics to predict vascular behavior", *Curr Opin Cardiol*, vol 18, 2003, pp: 458–470.

[6] P. H. Stone, A. U. Coskun, S. Kinlay, et al, "Regions of low endothelial shear stress are the sites where coronary plaque progresses and vascular remodelling occurs in humans: an in vivo serial study", *Eur Heart J*, vol 28, 2007, pp:705–710.

[7] S. Chien, S. Li, Y. J. Shyy, "Effects of mechanical forces on signal transduction and gene expression in endothelial cells", *Hypertension* vol 31, 1998, pp: 162-1698.

[8] P. F. Davies, "Flow-mediated endothelial mechanotransduction", *Physiol Rev*, vol 75, 1995, pp:519-5608..

[9] N. H. J. Pijls, B. de Bruyne, K. Peels, et al. "Measurement of fractional flow reserve to assess the functional severity of coronary-artery stenoses", *New Engl J Med* , vol 334, 1996, pp:1703–1708.

[10] R. K. Banerjee, L. H. Back, M. R. Back, Y. I. Cho, "Physiological flow simulation in residual human stenoses after coronary angioplasty", *Journal of Biomechanical Engineering*, vol 122, 2000, pp: 310-320.

[11] K. L. Gould, K. Lipscomb, G. W. Hamilton, "Physiologic basis for assessing critical coronary stenosis. Instantaneous flow response and regional distribution during coronary hyperemia as measures of coronary flow reserve", *Am J Cardiol, vol* 33 (1), 1974, pp: :87-94.

[12] H. V. Anderson, G. S. Roubin, P. P. Leimgruber, W. R. Cox, J. S. Jr. Douglas, S. B. King 3rd, A. R. Gruentzig, "Measurement of transstenotic pressure gradient during percutaneous transluminal coronary angioplasty", *Circulation*, vol 73(6), 1986, pp: 1223-1230.

[13] D. Bluestein, L. Niu, R. T. Schoephoerster, M. K. Dewanjee, "Fluid mechanics of arterial stenosis: Relationship to the development of mural thrombus", *Annals of biomechanical Engineering*, vol 25, 1997, pp: 344–56.

[14] M. Lei, J. P. Archie, C. Kleinstreuer, "Computational design of a bypass graft that minimize wall shear stress gradients in the region of the distal anastomosis", *Journal of Vascular Surgery*, vol l25, 1997, pp:637–46.

[15] D. Zeng, E. Boutsianis, M. Ammann, K. Boomsma, S. Wildermuth, D. Poulikakos, "A study of the compliance of a right coronary artery and its impact on wall shear stress", *Jurnal of Biomechanical Engineering*, vol 130, 2008, pp: 041014-11.

[16] G. A. Truskey, K. M. Barber, T. C. Robey, A. O. Lauri, M. P. Combs, "Characterization of a sudden expansion flow chamber to study the response of endothelium to flow recirculation", *Journal of Biomechanical Engineering*, vol 117, 1995, pp: 203-210.

[17] T. Karino, H. M. Herman, L. Goldsmith, "Particle flow behavior in models of branching vessels: I. Vortices in 90° T-junctions", *Biorhoelogy*, vol 16, 1979, pp: 231–4.

[18] W. F. Pritchard, P. F. Davis, Z. Derafsi, D. C. Polacek, R. Tsao, R. O. Dull, S. A. Jones, D. P. Giddens, "Effects of wall shear stress and fluid recirculation on the localization of circulating monocytes in a three-dimensional flow model", *Journal of Biomechanics*, vol 28(12), 1995, pp: 1459–69.

[19] A. Delfino, N. Stergiopulos, J. E. Jr. Moore, J. J. Meister, "Residual strain effects on the stress field in a thick-wall finite-element model of the human carotid bifurcation", *J. Biomech.,* vol 30, 1997, pp: 777–786.

[20] D. L. Fry, "Acute vascular endothelial changes associated with increased blood velocity gradients", *Circ. Res.*, vol 22, 1968, pp: 165–197.

[21] R. M. Nerem, "Vascular fluid mechanics, the arterial wall, and atherosclerosis", *J. Biomech. Eng.,* vol 114, 1992, pp: 274–282.